

An assessment of porosity and pore sizes in hardened cement pastes

N. McN. ALFORD, A. A. RAHMAN

*University of Oxford, Department of Metallurgy and Science of Materials,
Parks Road, Oxford, UK*

The porosity of hardened cement paste was analysed using fluid displacement methods, optical, scanning and transmission electron microscopy and mercury intrusion porosimetry. Attention has been drawn to the problems of mercury porosimetry and in particular to the extent of the pore volume which is missed by mercury. Previous workers have assigned the "lost porosity" to pore sizes too fine to be seen by mercury but this paper considers the contribution of closed pores. Nitrogen and water adsorption studies have been carried out on the pastes to determine qualitatively the magnitude of the pore volume beyond the range of mercury porosimetry. This volume was found to be very small. Emphasis has been placed upon the importance of large spherical pores, which may be missed by mercury porosimetry and adsorption studies, in determining the strength of cement pastes.

1. Introduction

Investigation of the porosity of cement paste has justifiably received considerable attention since porosity influences strength, permeability, durability, fracture toughness and elastic modulus of the paste. Young's modulus of cement paste is known to depend strongly on porosity and predictive equations of the type used by Hansen [1], Powers [2], Helmuth and Turk [3] and Hirsch [4] include porosity as one of the variables. Attempts to relate strength to total porosity have been met with only limited success, the reasons for which are described more fully elsewhere [5–7]. More recently, the emphasis of the investigations has been to analyse not simply the total pore volume but the pore-size distribution. Mikhail *et al.* [8] note "the sizes of pores have important effects on the technological properties of porous solids". The vital question is which size fractions are most important as far as cement is concerned.

Methods of analysing pore-size distribution include mercury intrusion porosimetry (MIP), adsorption studies and optical and electron microscopy. In this work no consideration has been given to such techniques as radiography, X-ray scattering and helium pycnometry or neutron-

derived porosity determinations. The purpose of this paper is to investigate critically the techniques, in particular MIP, commonly used and to determine their effectiveness in evaluating the porosity and pore-size distribution of a sample. Finally, suggestions are made as to the best methods of evaluating the complete pore-size distribution in a cement paste.

The main concern of the authors is the macroporous region of cement paste and, since MIP is the technique most commonly used in the evaluation of cement macroporosity, considerable attention has been devoted to this method and its limitations in this work. The MIP method has been frequently used to analyse the pore characteristics of hardened cement pastes [9–15] and the accuracy of the method is governed by that of the porosimeter. Most commercial instruments have a pressure range reaching 200 MPa although some porosimeters are capable of working to pressures slightly in excess of 400 MPa, i.e., are capable of detecting a pore diameter of approximately 2.0 nm. The upper diameter may be extended in theory to approximately 1 mm by applying a vacuum pressure on the filling device of the instrument.

TABLE I Pore analysis data

Sample number	w:c ratio	Age (days)	Hg volume intruded ($\text{cm}^3 \text{g}^{-1}$)	Volume intruded (%)	Pore volume ($\text{cm}^3 \text{g}^{-1}$)	Total porosity (%)
1a (compact)	< 0.15	3	0.044	58.7	0.075	18.0
1b (compact)	< 0.15	8	0.036	48.0	0.075	18.0
1c (compact)	< 0.15	34	0.033	47.1	0.070	17.5
2a	0.25	3	0.131	70.4	0.186	33.5
2b	0.25	8	0.093	50.8	0.183	33.0
2c	0.25	34	0.083	45.3	0.183	33.0
3a	0.3	5	0.133	70.8	0.188	34.3
3b	0.3	11	0.116	61.9	0.187	34.0
3c	0.3	34	0.1044	57.0	0.182	33.0
4a	0.35	6	0.170	73.3	0.232	39.2
4b	0.35	10	0.155	69.2	0.224	38.0
4c	0.35	21	0.136	68.0	0.200	35.1
5a	0.6	4	0.335	76.2	0.440	55.0
5b	0.6	22	0.278	64.5	0.431	52.0
5c	0.6	36	0.251	60.9	0.412	50.1
6a	0.8	4	0.489	86.5	0.565	62.1
6b	0.8	22	0.449	85.2	0.527	58.0
6c	0.8	36	0.425	81.6	0.521	56.0

Low-pressure and conventional pressured MIP have always been subject to two major problems. First, the pore diameters recorded are not necessarily the true pore diameters but are the pore entry diameters. Second, there exists the problem of the "lost porosity", i.e., the mercury appears to be unable to reach the total pore space of the sample. In addition there are the usual problems concerned with the choice of contact angle and the degree of sample damage. Diamond [10] noted that neither MIP nor capillary condensation techniques appeared capable of recording all the pore space in a given sample. Previously, Winslow and Diamond [9] and other workers had ascribed the lost porosity to pores which were too fine to be measured by MIP. Diamond later suggested [10] that the lost porosity might not be in the ultra-fine pores but in "encapsulated pockets of gel" which would be unintrudable by mercury at any pressure. Beaudoin [12] showed that mercury cannot enter all the pore space available to helium and suggested the existence of micro-space between aggregations of C-S-H sheets accessible to helium but not to mercury. In this paper by Winslow and Diamond [9] the discrepancy between the mercury volume intruded and the total pore volume in the cement paste was attributed to ultra-fine pores. If we take a typical cement paste such as the one given by Winslow and Diamond in Table I [9]: 28 days old with a

water:cement (w:c) ratio of 0.4 it is seen that 35% of the pore volume is unintruded. This 35% is therefore ascribed to pores too fine to be intruded by mercury or in a later interpretation mentioned above [10] in encapsulated pockets of gel.

It is our suggestion that only part of the lost porosity may be ascribed to the fine end of the pore-size distribution, the remainder being found in large voids enclosed by pores too fine to be recorded by MIP. In order to gain quantitative information concerning pores with diameter greater than $15 \mu\text{m}$, low-pressure porosimetry is conventionally used. However, this necessarily assumes a perfectly inter-connecting pore system in which all the pores above $15 \mu\text{m}$ in diameter are connected by pore channels of gradually decreasing size, whereby the first pores to come into contact with the mercury are the largest and subsequent pores are progressively smaller. Fig. 1a shows a system where low-pressure porosimetry would produce reliable results. Fig. 1b, c and d show systems where low-pressure porosimetry would produce erroneous results.

In the case of Fig. 1b the mercury would only "see" the first large opening and interpret the second large opening as the diameter of the connecting channel, i.e., the pore entry diameter. In the case of Fig. 1c the large spherical pore is connected by pore channels which are too fine to

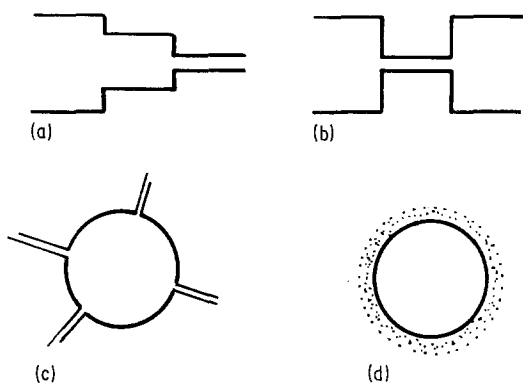


Figure 1 Schematic representation of variation in pore types.

admit mercury under the maximum pressure available and this spherical pore is missed entirely, contributing therefore to the lost porosity. Fig. 1d is a special case of Fig. 1c in that the large spherical void is surrounded by products of hydration which are too fine and closely-packed to be intruded by mercury.

The experimental work in the next section describes the attempts made to resolve the problem of the lost porosity and the pore distribution in cement pastes.

2. Experimental methods

A series of OPC Type 1 pastes were prepared with varying w:c ratios producing pastes with a wide range of total porosities. A second series of pastes were subjected to compaction in a stainless steel compaction jig in order to reduce the total porosities [16]. A third series was made with an addition of 0.1 and 0.2 wt % of aluminium powder in order to aerate the sample. The pastes were tested by MIP assuming a contact angle of 140° . The pastes were oven dried at 105°C for 24 h and then transferred to a desiccator for cooling. Replicate specimens were tested for total porosity using a water immersion method [17] and a kerosene immersion method. A further consideration of the details of the measurement of total porosity using different methods is made later in the text. The specimens were examined by optical microscopy (OM) where the pore sizes in excess of $15\ \mu\text{m}$ diameter were counted in a series of transverses across the polished surface of the sample. Scanning and transmission electron microscopy was used to determine qualitatively the abundance of pores below $15\ \mu\text{m}$ diameter. Three sets of samples of

widely varying total porosities were subjected to both nitrogen and water adsorption studies.

3. Results

3.1. Mercury intrusion porosimetry

Table I gives the pore characteristics of the samples tested. Total porosity was measured by water immersion and this has been noted by some workers [2, 15, 18] to give slightly higher total porosities than if measured by helium, paraffin, neutron scattering, acetone or toluene methods. In fact, all these methods give different total pore volumes. Sereda *et al.* [15] observe that the difference between methanol and water porosity is about 8% and that helium porosity is very close to the porosity as measured by methanol. In the present study porosities measured by immersion in paraffin showed a difference of about 10% in the total porosity.

Powers [19] noted that liquid displacement using acetone, carbon tetrachloride and toluene also gave slightly lower results and ascribed this difference to molecular size effects and the difference in specificity of interaction between the solid and the respective liquids. While the authors are aware of this discrepancy it does not affect the conclusions reached here, although it does reduce the amount of lost porosity by a few per cent.

It was observed that after a period of 3 days the total porosities of the samples varied only slightly with time suggesting that changes in porosity after 3 days were confined to the fine end of the pore-size distribution (see Table I). That this was the case was endorsed by observations that there was a considerable decrease in the intruded mercury volume with time. This is indicated in Table I and in Figs 2 and 3. It was also noted that in the high w:c ratio (0.8) samples the mercury volume intruded after only four days was high (86.7%). This was reduced to 81.7% after 36 days, still a high percentage intrusion which is most probably due to the highly open structure of the paste at such high w:c ratios.

The gradual reduction of the intruded mercury volume is consistent with micro- and possibly meso-pores being infilled with the products of hydration. Fig. 3 shows the effect of w:c ratio on the maximum mercury volume intruded with time. It is interesting to observe the change in shape of these curves with increasing w:c ratio, the changes being indicative of the degree of infilling by the hydration products. Thus the change in slope for

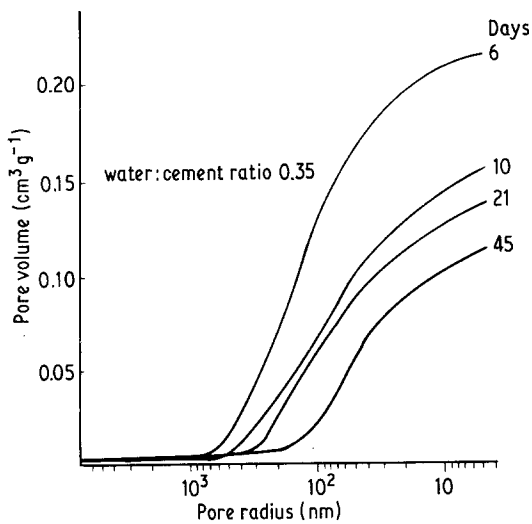


Figure 2 Cumulative Hg volume intruded with time.

a compacted sample is less than that of a high w:c ratio paste which possesses a more open structure capable of accommodating the products of hydration. These are likely to be greater for high w:c ratio samples than for low w:c ratio pastes and compacted samples where hydration may be reduced and where the space available for hydration products is less.

Three series of samples were chosen for low-pressure porosimetry, the results of which are given in Table II.

In the sample prepared with 0.10 wt% Al powder, the channels produced are such that down to a diameter of 15 μm , 29.78% of the total pore volume has been intruded. Below 15 μm diameter 55.3% of the pore volume is intruded. A combi-

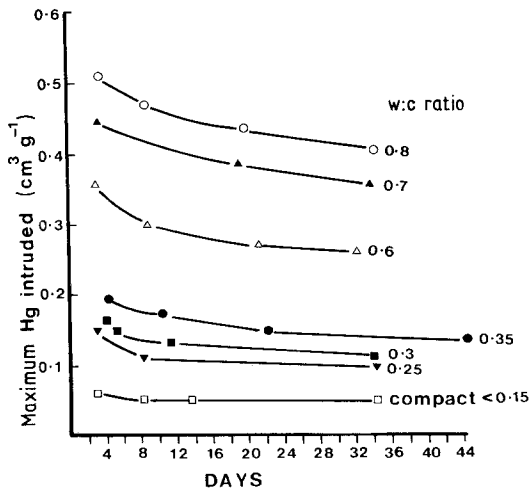


Figure 3 Maximum Hg volume intruded with time.

nation of these two values leaves 14.92% of the pore volume "unseen" by mercury. This sample presented favourable considerations for MIP possessing a large volume of interconnecting pore channels (Fig. 5c).

In the untreated pastes the situation is different. There are certainly interconnecting channels in the case of 0.8 w:c ratio paste but only 1.43% of the total pore volume has been intruded by mercury into pores greater than 15 μm diameter. Total mercury intrusion was 81.73% from which it was deduced that in high w:c ratio pastes with open pore structures the pore-type conformed to that shown in Fig. 1b, although 18.27% of the pore volume was still missed. At w:c ratio of 0.3 only 1.07% of the pore volume is intruded at pores greater than 15 μm , 61.9% of the pore volume is intruded by mercury under pressure leaving a total unintruded volume of 37.03%. It is seen that, with the exception of the aluminium-treated pastes, the volume of mercury intruded into pores greater than 15 μm diameter by mercury under low pressure is very small. The cylindrical pore-type shown in Fig. 1a does not apply to these pastes. The pore-types shown in Fig. 1b and c predominate in high w:c ratio pastes with a high degree of interconnectivity. In low w:c ratio and compacted pastes many of the small tributary channels are not filled even at high pressure and in these cases the magnitude of unintruded pore volume is increased (see Table I) and the predominant pore-types are most probably a combination of those shown in Fig. 1c and d.

Fig. 4 shows the results of the low-pressure porosimetry where it is seen that only the aluminium-treated paste shows any significant intrusion by mercury.

3.2. Optical and electron microscopy

The surfaces of the pastes revealed a large number of spherical voids of size in excess of 15 μm , as shown in Fig. 5a and b.

The photomicrographs shown in Fig. 5a and b indicate the presence of spherical voids, some of size in excess of 2 mm, in abundance throughout the paste. If it is accepted that these voids do exist then the validity of low-pressure MIP results must be questionable. At best, only the pores on the surface of the sample will be "seen" and these pores form only a small fraction of the large pores throughout the sample. Quantitative optical microscopy on representative samples revealed a

TABLE II Low-pressure MIP data

Sample number	Age (days)	w:c ratio	Pore volume ($\text{cm}^3 \text{g}^{-1}$)	Total porosity (%)	Hg volume intruded ($\text{cm}^3 \text{g}^{-1}$)		Pore volume intruded (%)		Density (g cm^{-3})
					MIP	Low-pressure MIP	MIP	Low-pressure MIP	
7	9	0.3	0.187	34.2	0.116	0.002	61.9	1.07	1.83
8 (Al)	9	0.3	0.329	46.0	0.182	0.098	55.3	29.78	1.40
9	9	0.8	0.560	61.6	0.45	0.008	80.3	1.43	1.10

large discrepancy between the volume-fractions of pores in excess of $15 \mu\text{m}$ recorded by low-pressure MIP and the volume-fraction of pores counted by optical microscope (OM) methods. Fig. 6a, b and c shows the percentage porosity, measured using optical microscopy, for aluminium-treated pastes, for pastes of w:c ratio 0.3 and for compacted pastes, respectively. Even in compacted pastes, pores with an average diameter of $125 \mu\text{m}$ were counted. In uncompact pastes pores of diameter up to $325 \mu\text{m}$ were observed and, in the aluminium-treated pastes and pastes with w:c ratio of 0.3, channels of width up to $650 \mu\text{m}$ could be seen with a mean width of about $100 \mu\text{m}$, as shown in Fig. 5c. It will be noted from Table III that the pore volumes counted by OM and MIP methods combine to give a value in excess of the total pore volume of the sample. This may be explained by a certain degree of overlap between the two methods in that some of the pores counted by OM in excess of $15 \mu\text{m}$ will be filled by mercury at high pressures corresponding to a pore entry diameter less than the true diameter of the pore. The effect

of this would be to increase artificially the pore volume measured by the combination of the two techniques.

The contribution to the total pore volume of pores of diameter greater than $15 \mu\text{m}$ is seen to be considerable. Fig. 7 shows the combination of MIP data with optical microscopy data and it will be noted that there is a "plateau" region which becomes more extensive as the pore volume of the sample decreases. It is believed that the plateau is an artefact caused by the mode of mercury intrusion, discarding as it does all pores within the size range $15 \mu\text{m}$ to 40nm for compacted samples, $15 \mu\text{m}$ to 70nm for uncompact samples and $15 \mu\text{m}$ to 500nm for aluminium-treated samples. The plateau region ends with a fairly sharp increase in the slope of the cumulative curve which represents not an abundance of pores at this increase but a pore entry diameter where the mercury is finally able to begin invading the sample. It is more likely that true form of the cumulative curve possesses no such sharp increase but that there is a smooth continuation of the curve leading up to the final pore volume of mercury intruded. The pore entry diameter will diminish as hydration products begin to in-fill the pores, as shown in Fig. 8a.

Supporting evidence for the existence of pores within the plateau region is seen in the TEM and SEM photomicrographs shown in Fig. 8b and c. It was hoped to perform similar quantitative work on pores of size less than $15 \mu\text{m}$ but quite early on in the investigation it became apparent that, although qualitative information was readily available, any attempt to quantify pore volumes in classes below $15 \mu\text{m}$ would be statistically unreliable.

3.3. Adsorption studies

It remains to determine the extent of the pore volume of pore-size below the range of the porosimeter, which is where much of the lost

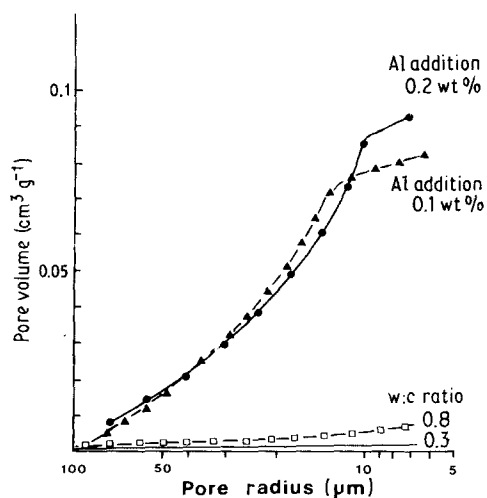


Figure 4 Cumulative volume intruded using low-pressure mercury porosimetry.

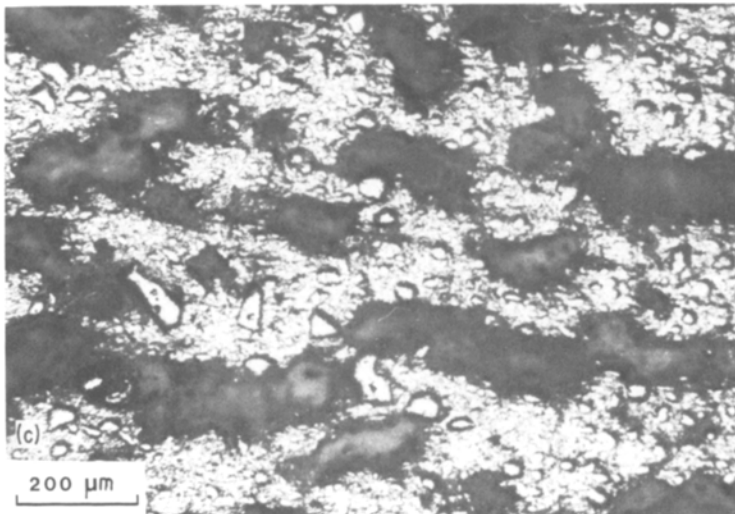
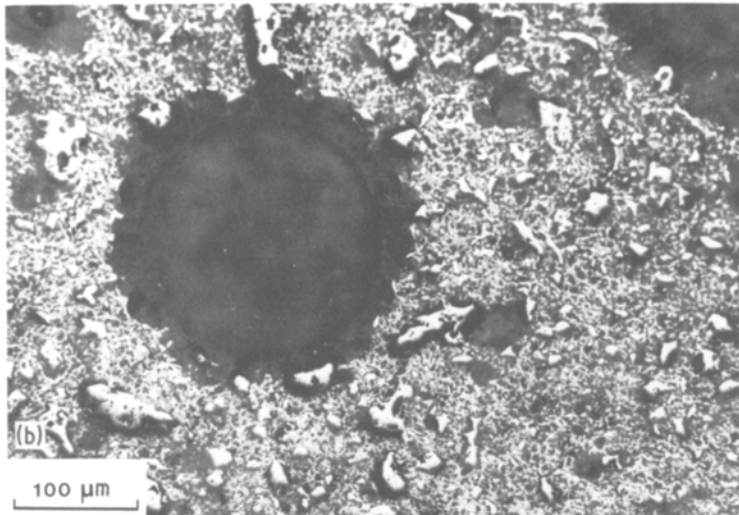
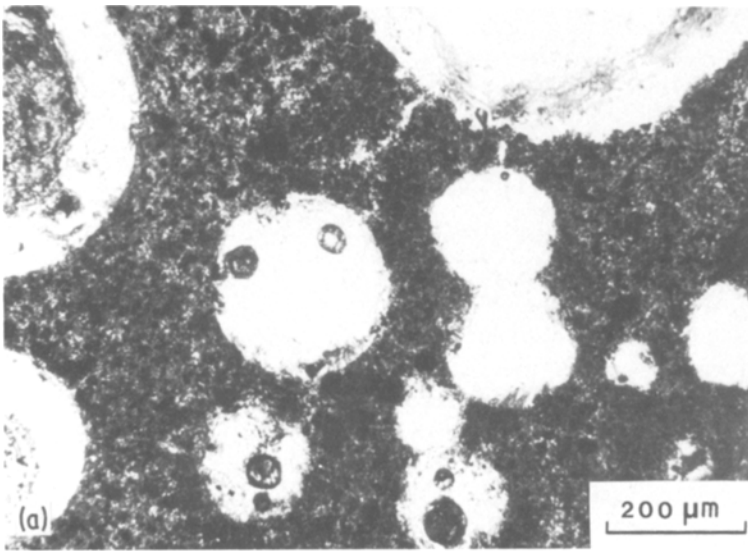


Figure 5 Optical micrographs of samples: (a) Abundance of large spherical pores of varying sizes and pore coalescence in sample of w:c ratio 0.8 (transmission); (b) Polished section of sample of w:c ratio 0.4 showing large spherical voids surrounded by smaller voids; (c) Polished section of aluminium-treated paste showing pore channel system.

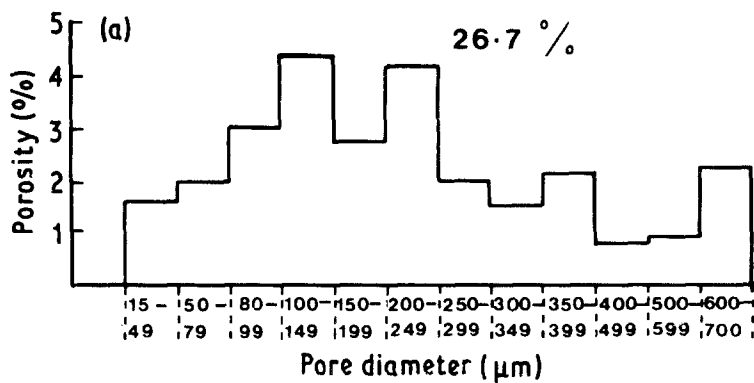
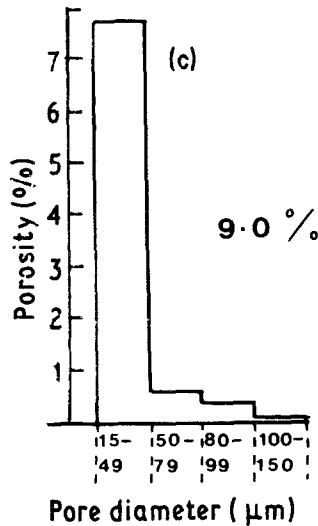
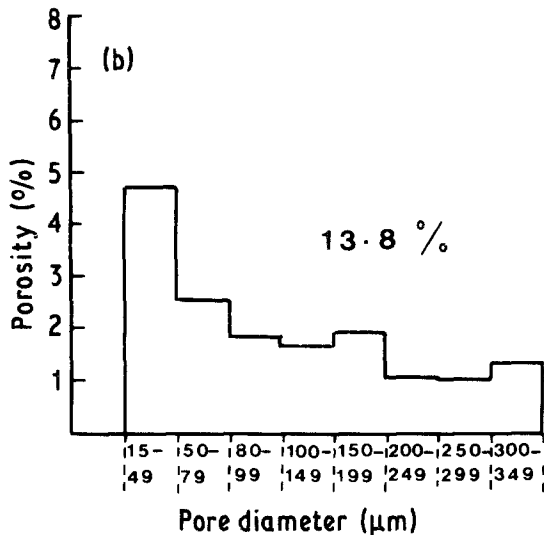


Figure 6 Histograms of percentage porosity against pore diameter ranges for different samples. (a) Sample 10, Al treated paste: total porosity = 46.0%, porosity counted by OM = 26.7%. (b) Sample 11, paste with w:c ratio of 0.3: total porosity = 34.6%, porosity counted by OM = 13.8%. (c) Sample 12, compact paste with w:c ratio of <0.15: total porosity = 15.54%, porosity counted by OM = 9.0%.



porosity has been assumed to exist. In the first instance, if one combines the pore volumes counted by optical microscopy and MIP (Table III) it would appear that very little pore volume exists below the range of MIP although a considerable amount lies above this range. Water and nitrogen adsorption studies were performed on compacted, w:c ratio 0.3 and w:c ratio 0.8 samples of paste in order to determine, at least qualitatively, the extent of the pore volume with pore-size below approximately 50 nm. The isotherms shown in Fig. 9a and b are representative of the samples tested.

The isotherms appear to be representative of a

Type II isotherm [20]. The hysteresis loops conform to a Type B in the case of nitrogen, modified to Type D in the case of water [21]. Only a small proportion of the nitrogen and water is adsorbed in the initial part of the isotherm, indicating the absence of much micro-porosity. The asymptotic nature of the curves suggests the existence of a pore volume beyond the upper limit of nitrogen and water adsorption. The conclusion reached on the use of adsorption isotherms as a means of characterizing the porosity of cement paste is that they are inadequate simply because these methods can only describe pore sizes up to 50 nm. Some authors [10, 22] are of the opinion that capillary

TABLE III Total pore volume measured by water immersion and pore volumes measured by MIP and OM

Sample number	w:c ratio	Total pore volume (cm ³ g ⁻¹)	Hg intruded volume (cm ³ g ⁻¹)	OM pore volume counted (cm ³ g ⁻¹)	Total OM and MIP volume (cm ³ g ⁻¹)	Combined volumes (%)
10 (Al)	0.3	0.328	0.182	0.198	0.379	115.5
11	0.3	0.178	0.115	0.082	0.197	110.7
12 (compact)	<0.5	0.062	0.036	0.035	0.071	114.5

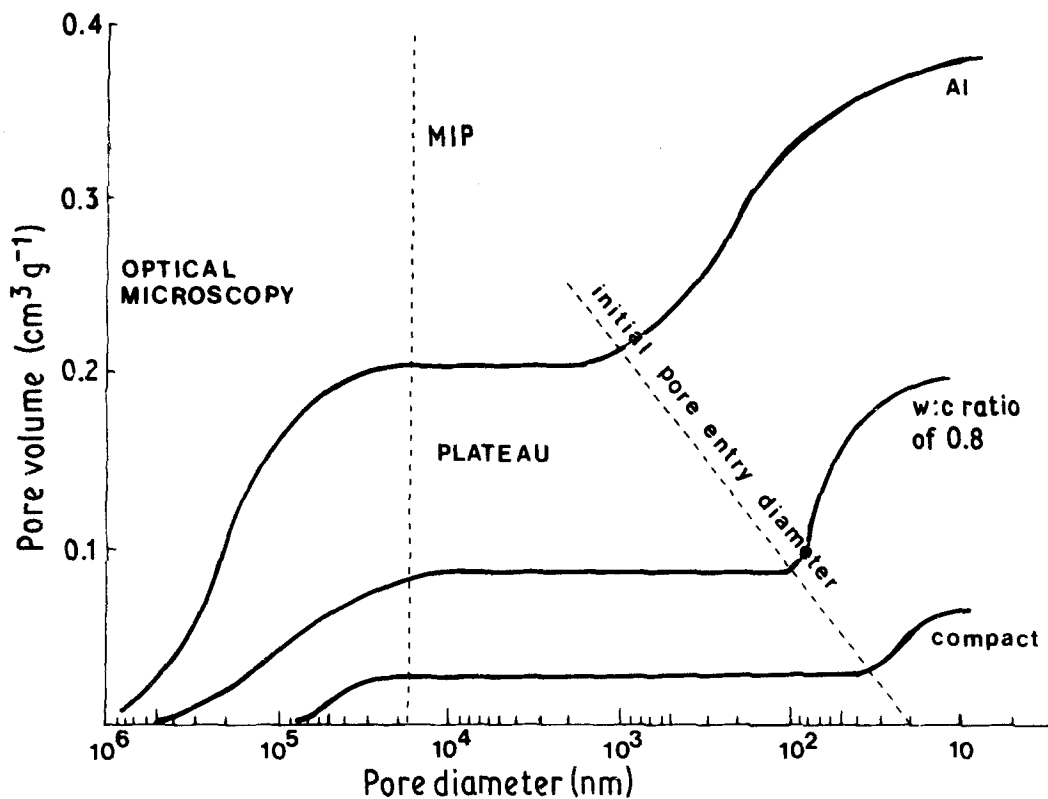


Figure 7 Cumulative pore volumes counted by optical microscopy and mercury intrusion porosimetry.

condensation measurements can be untrustworthy even for pore diameters below 8 nm and are liable to give unreliable pore-size distributions in this region.

The present writers believe that the pore volume measured by adsorption methods must be very small indeed for two reasons. The first is that the nature of the isotherms themselves preclude any significant pore volume below the range of MIP. The second is that a combination of MIP data and optical microscopy accounts for what seems to be nearly all the pore volume even allowing for overlap between OM and MIP. This raises doubts as to the average diameter of the pores in cement paste. Winslow and Diamond [9] give the average diameter in a 1 day old paste, of w:c ratio 0.6, as 300 nm, which drops to 10 nm after one week. This was determined, as Diamond later explained [10], by using the "volume mean diameter" which is that diameter above and below which lies 50% of the pore volume. Mikhail *et al.* [8] calculated an average diameter of 4.72 nm for a cylindrical pore with length 46.6 nm using radius of gyration plus the hydraulic radius. Whether the term average pore or volume mean diameter is

used the concept appears to lack any reality. For example, the volume of one spherical pore of diameter 500 μm is equivalent to the combined volumes of 1.25×10^{14} spherical pores of diameter 10 nm. The distribution of pore sizes in cement is not Gaussian and is strictly-speaking incapable of being characterized by a statistic such as the mean. If a volume mean diameter approach is used in this work then the average pore would be between 500 nm and 5 μm . This begins to have practical significance if we revert to the original question as to which size ranges have the most important effects on the technological properties of cement paste.

As far as elastic modulus is concerned the volume-fraction of pores still appears to exert a considerable influence, although recent work [5] would indicate that this is not so simple a relation as has been previously supposed. Similarly, durability and permeability are dependent both on volume-fraction, pore size and the degree of pore linkage. The strength of cement paste has been shown [5-7] to depend primarily, not on volume-fraction of pores, but on pore size. In this case it is the larger pore acting as a Griffith flaw which

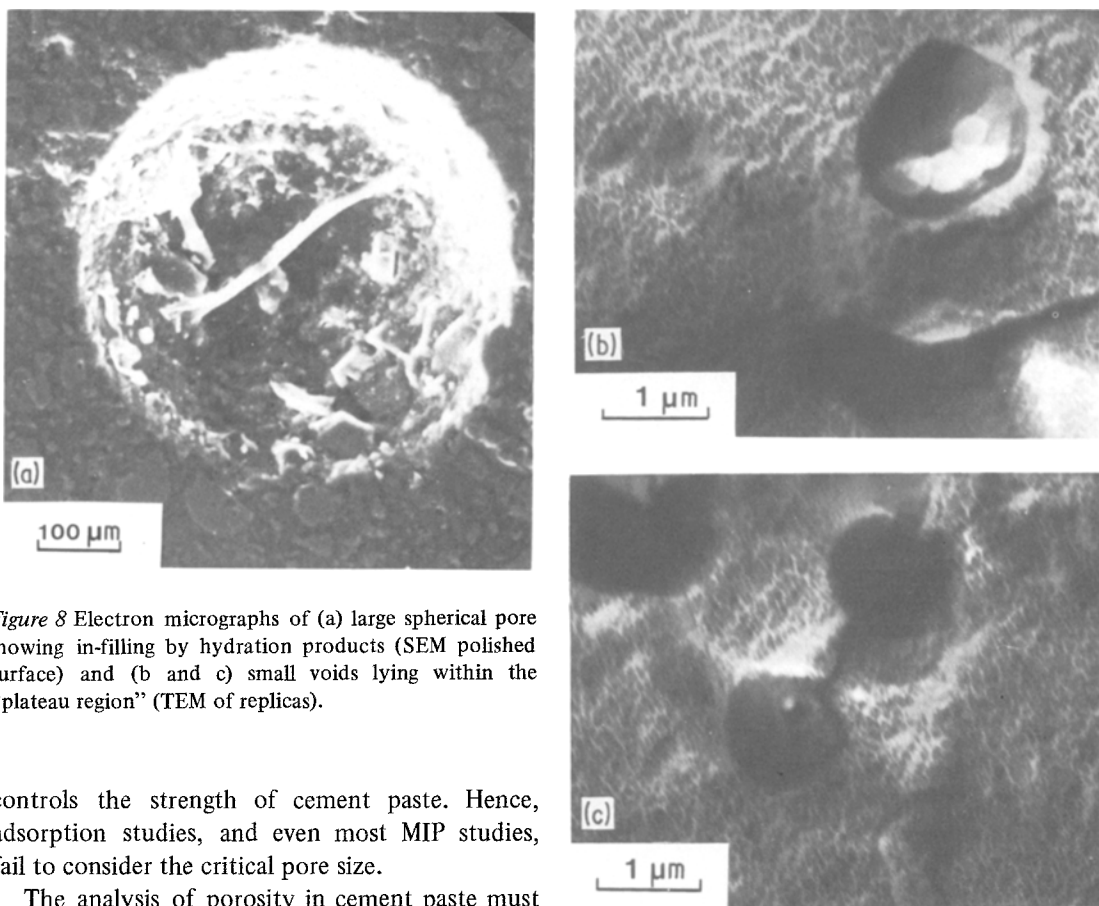


Figure 8 Electron micrographs of (a) large spherical pore showing in-filling by hydration products (SEM polished surface) and (b and c) small voids lying within the “plateau region” (TEM of replicas).

controls the strength of cement paste. Hence, adsorption studies, and even most MIP studies, fail to consider the critical pore size.

The analysis of porosity in cement paste must be approached in a number of different ways. First, the pore volume of the sample must be determined and the techniques available have been described above. Then the pores in excess of $15\ \mu\text{m}$ diameter should be point-counted using optical microscopy (this diameter could be reduced to about $5\ \mu\text{m}$ if desired). MIP methods can be used to determine pore diameters between $15\ \mu\text{m}$ and about $4\ \text{nm}$, bearing in mind that the distribution of porosity will depend on the pore entry diameter. Adsorption methods may be used for pores of diameter below $4\ \text{nm}$ but the contribution at these pore sizes is very small indeed and the pore-size distributions so obtained are of questionable validity.

4. Summary and conclusions

(a) MIP does not measure the total pore volume in hardened cement paste. Optical microscopy reveals that between 30 and 50% of the pore volume may be found in pores in excess of $15\ \mu\text{m}$ diameter.

(b) The “lost porosity” (i.e., that pore volume missed by MIP) is considered to exist predomi-

nantly in spherical macropores. Most of the lost porosity is probably due to the presence of pores of the type shown in Fig. 1c and d.

(c) Adsorption studies indicate that the amount of porosity below the range of MIP detection (less than about $4\ \text{nm}$ radius) is very small and cannot account for the total lost porosity.

(d) The plateau region observed in MIP cumulative pore volume curves most probably does not exist and is a function of the pore entry diameter. SEM and TEM studies reveal the presence of pores within the plateau region.

(e) Although MIP alone does not adequately characterize the total pore volume or pore-size distribution of cement pastes, microstructural changes in the paste are reflected by changes in MIP data. For example, ageing, changes in water : cement ratio, introduction of air entraining agents, use of chemical admixtures [16] and compaction will drastically alter the data output and extreme care must be taken in the interpretation of the results so obtained.

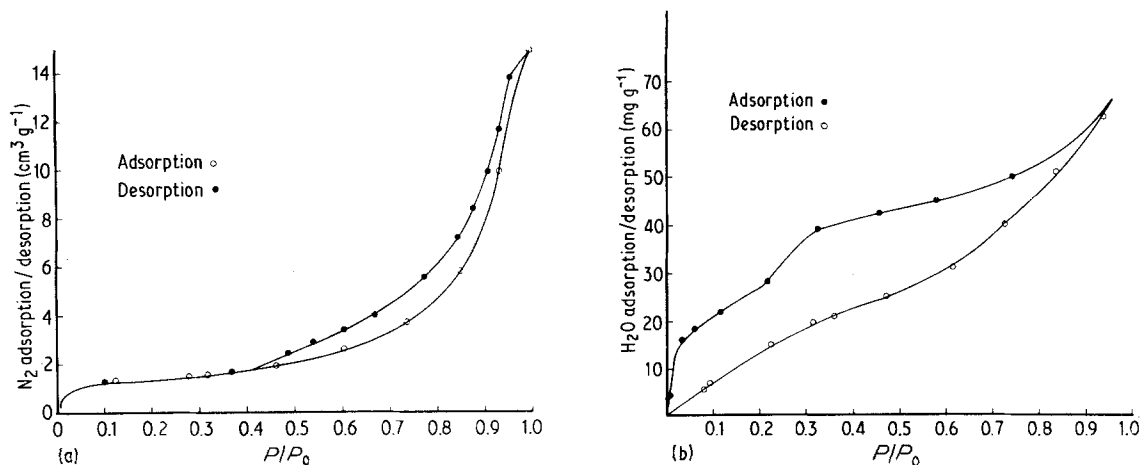


Figure 9 (a) N_2 volume adsorption isotherm and hysteresis curve, measured at NTP; (b) H_2O weight adsorption isotherm and hysteresis curve.

Acknowledgements

The authors wish to thank Imperial Chemical Industries Limited (NMcNA) and the Science Research Council (AAR) for financial assistance. Thanks are also due to Dr D. D. Double for helpful discussions, to Mr N. Salih for technical assistance and advice and to Professor K. S. W. Sing of Brunel University for the use of adsorption apparatus. The TEM micrographs were taken by Mr P. Johnson for which the authors are most grateful.

References

1. T. C. HANSEN, *J. Amer. Concrete Inst. Proc.* **62** (1965) 193.
2. T. C. POWERS, "Fundamental Aspects of Shrinkage of Concrete" *Revue des Materiaux* Number 544 (1961) p. 79.
3. R. A. HELMUTH and D. H. TURK, Symposium on the Structure of Portland Cement Pastes and Concrete, National Research Council, Highway Research Board Special Report Number 90, Publication Number 1389 (Highway Research Board, Washington, DC, 1966) p. 135.
4. T. J. HIRSCH, *J. Amer. Concrete Inst. Proc.* **59** (1959) 427.
5. J. D. BIRCHALL, A. J. HOWARD and K. KENDALL, *Nature* **289** (1981) 388.
6. European Patent Publication No. 002 1682, Imperial Chemical Industries Ltd (1981).
7. N. McN. ALFORD, *Cement Concrete Res.*, to be published.
8. R. Sh. MIKHAIL, D. H. TURK and S. BRUNAUER, *Cement Concrete Res.* **5** (1975) 433.
9. D. N. WINSLOW and S. DIAMOND, *J. Mater.* **5** (1970) 564.
10. S. DIAMOND, *Cement Concrete Res.* **1** (1971) 531.
11. E. J. SELLEVOLD, *ibid.* **4** (1974) 399.
12. J. J. BEAUDOIN, *ibid.* **9** (1979) 771.
13. D. H. BAGER and E. J. SELLEVOLD, *ibid.* **5** (1975) 171.
14. D. A. KAYALI, C. L. PAGE and A. G. B. RITCHIE, Proceedings of the Conference on Hydraulic Cement Pastes: Their Structure and Properties, Sheffield April 1976 (Cement and Concrete Association, Slough, 1976) p. 204.
15. P. J. SEREDA, R. F. FELDMAN and V. S. RAMACHANDRAN, Proceedings of the 7th International Congress on the Chemistry of Cement, Paris, 1980, Vol. I, p. VI-1/3.
16. N. McN. ALFORD, A. A. RAHMAN and N. SALIH, *Cement Concrete Res.* **11** (1981) 235.
17. N. McN. ALFORD and A. B. POOLE, *Cement Concrete Res.* **10** (1980) 263.
18. D. H. C. HARRIS, C. G. WINDSOR and C. D. LAWRENCE, *Mag. Concr. Res.* **26** (1974) 65.
19. T. C. POWERS and T. L. BROWNYARD, *Res. Dev. Bull. Portland Cement Assoc.* **22** (1948) 692.
20. S. BRUNAUER, L. S. DEMING, W. W. DEMING and E. TELLER, *J. Amer. Chem. Soc.* **62** (1940) 1723.
21. D. H. EVERETT, "The Gas-Solid Interface" Vol. 2, edited by E. A. Flood (Edward Arnold, London, 1967) p. 1055.
22. M. M. DUBININ, in "Progress in Surface and Membrane Science" Vol. 9, edited by D. A. Cadenhead, J. F. Danielli and M. D. Rosenberg (Academic Press, New York and London, 1975) p. 1.

Received 19 March and accepted 13 April 1981.